

# Temperature and excitation density dependence of the photoluminescence from annealed InAs/GaAs quantum dots

E. C. Le Ru\*, J. Fack, and R. Murray

*Centre for Electronic Materials and Devices, Imperial College, London SW7 2BZ, United Kingdom*

(Received 18 September 2002; published 23 June 2003)

Using rapid thermal annealing, we fabricated a series of InAs/GaAs quantum dot samples with ground-state emission ranging from 1.05 eV to 1.35 eV. This set of annealed samples, all having the same density, allows us to study the influence of the barrier height on the temperature dependence of the photoluminescence (PL). The integrated PL follows an Arrhenius-type behavior, with activation energies matching the barrier heights. However, the quenching occurs at lower temperatures as the barrier height decreases. The modeling of these data enables us to understand the important mechanisms determining the critical temperature where the quenching occurs. We also present a detailed investigation into the excitation density dependence of the photoluminescence at different temperatures. Under relatively low excitation, this dependence is linear at 10 K, and becomes increasingly superlinear and eventually quadratic as the temperature is increased and carriers escape from the dots. However, under high excitation, the dependence remains linear even at high temperatures and the activation energy for quenching is different. We show that all these results can be understood by considering the independent capture and escape of electrons and holes in the dots.

DOI: 10.1103/PhysRevB.67.245318

PACS number(s): 78.67.Hc, 73.21.La, 78.55.Cr, 71.38.-k

## I. INTRODUCTION

Self-assembled quantum dots (QD's) are predicted to replace quantum wells (QW's) as the active layer of many optical and electro-optical devices. Three-dimensional confinement of carriers leads to unique properties such as a  $\delta$ -like density of states and ultranarrow homogeneous broadening. In principle, QD lasers should have very low threshold currents and improved critical temperatures. The devices fabricated so far have not yet met these expectations and many issues remain to be understood. Among these, the behavior at high temperature is of great importance because most devices operate at room temperature or higher.

There are two main features in the temperature dependence of QD's. First, most studies<sup>1-10</sup> report a quenching of the photoluminescence (PL) intensity with increasing temperature. This is usually attributed to thermal escape of carriers from the dots into the barrier material,<sup>1-9</sup> where they are lost through, for example, nonradiative recombination.<sup>5,10</sup> Our results confirm this, but also show that the critical temperature where the quenching occurs increases with the barrier height and changes with excitation density. The second feature is the variation of the emission energy and the full width at half maximum (FWHM), which have also been extensively investigated.<sup>2,4,7,8</sup> A decrease of the FWHM, together with a red shift of the emission wavelength is usually observed in the midtemperature range. These features are explained by thermal escape occurring at lower temperatures for high-energy dots and carriers being recaptured by dots emitting on the low-energy side of the distribution. Numerical models support these explanations.<sup>8</sup> In the previous studies, the effect of the excitation density was often overlooked, or the dependence was shown to be linear at all temperatures.<sup>6</sup> A superlinear behavior was reported in Ref. 9 above room temperature and attributed to saturation of losses in the barrier.

In this paper, we study the temperature and excitation density dependence of the PL of four samples obtained by

rapid thermal annealing from the same piece of wafer. These four samples therefore have some common properties (like the density of dots), but different electronic levels. By comparing the behavior of each of them with temperature, it is possible to clarify the mechanisms that contribute to the observed temperature dependence. Moreover, these samples have relatively narrow FWHM, which makes the interpretations easier and more reliable. For each sample, we studied the temperature dependence of the integrated PL intensity (IPL) and analyzed the results using a simple rate equation model. Similar behavior to that already reported was observed, but the comparison between samples gives new insights into their physical origin. We also studied in detail the excitation dependence of the IPL at different temperatures. A strong superlinearity is observed under certain conditions, namely, high temperatures and low excitations. We believe this observation is important for an understanding of the temperature dependence and discuss its possible origin. The analysis of the series of experimental results presented here suggests that this effect is due to the independent escape and capture of electrons and holes. An important consequence is that the temperature dependence of the PL from QD's can vary a lot depending on the excitation density, which can account for the variety of different observations reported so far.

The paper is organized as follows: we will first describe in Sec. II the samples studied here and the experimental details. In Sec. III, we discuss and model the dependence of the integrated PL with temperature, focusing on the effect of the barrier height of the dots. In Sec. IV, we focus on the superlinear dependence of the IPL with excitation density. We present a series of experimental results characterizing this effect, and discuss the possible explanations of this phenomenon and the consequences of these results.

## II. EXPERIMENTAL DETAILS

The parent sample A was grown using conventional solid source molecular-beam epitaxy but with the InAs layer de-

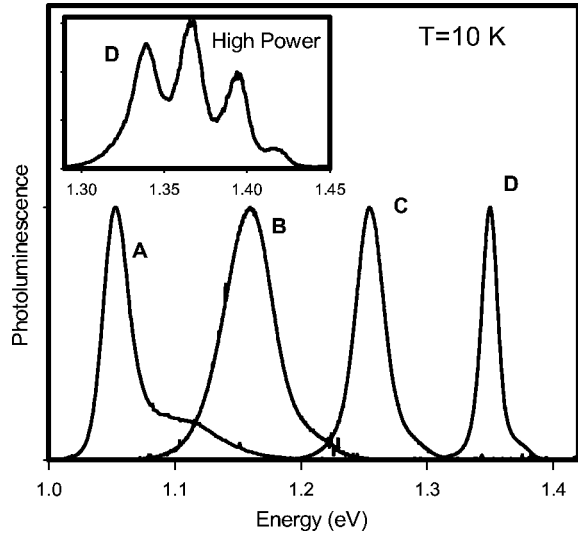


FIG. 1. Low temperature, low excitation PL spectra from the as-grown sample (A) and samples annealed at 650 °C (B), 700 °C (C), and 750 °C (D) for 10 s. The inset shows high excitation spectra from sample D. The excited states are well defined, showing that the annealed samples retain their dotlike characteristics.

posited at a low-growth rate [ $\leq 0.01$  monolayer per second (ML/s)]. This results in emission close to 1.3  $\mu\text{m}$  at room temperature (1.047 eV at 10 K for this sample), combined with a very small inhomogeneous broadening (25 meV).<sup>11</sup> A six-period AlAs/GaAs  $6 \times 6$  ML superlattice was grown 10 nm before the QD layer and 20 nm above. Such a superlattice is very important for temperature studies, because it confines the carriers to a known GaAs region. In this way, carrier diffusion along the growth direction in the GaAs surrounding the dots does not need to be taken into account in the analysis.

The height of the barrier  $E_b$  is taken to be the difference between the GaAs band gap and the emission energy of the ground state (GS), and is thus equal to 462 meV for sample A. This barrier is quite high compared to samples studied in previous works. To study the influence of the barrier height, we used rapid thermal annealing (RTA) at different temperatures to produce three other samples. It has been shown previously that RTA induces indium/gallium interdiffusion, thus having the effect of blue shifting the GS energy, and therefore decreasing the barrier height,<sup>9,12,13</sup> while keeping other important properties, such as the QD density, exactly identical. Pieces of sample A were capped with 100 nm of SiO<sub>2</sub> and subjected to 10-s anneals in an argon atmosphere in a rapid thermal annealer at a temperature of 650 °C (B), 700 °C (C), or 750 °C (D). Figure 1 shows the emission obtained at low excitation for all the samples after removal of the SiO<sub>2</sub> cap. The inset shows the emission from sample D under high excitation and demonstrates clear level filling indicating that the dot characteristics are retained after annealing. All the samples exhibit emission from several excited states with a constant intersublevel spacing. The transition energies of the ground state  $E_{GS}$ , intersublevel spacing  $\Delta E$ , and FWHM of the GS are summarized in Table I. These annealed samples have barrier heights of 358 meV (B), 261

TABLE I. Characteristics of the QD samples used in this study, as measured from various PL experiments: GS energy  $E_{GS}$ , intersublevel spacing  $\Delta E$ , FWHM of the GS, WL emission energy  $E_{WL}$ , barrier height  $E_b$ ,  $\ln(C_{exp})$  (see text), and radiative lifetime  $\tau$ .

	$E_{GS}$ (eV)	$\Delta E$ (meV)	FWHM of GS (meV)	$E_{WL}$ (eV)	$E_b$ (meV)	$\ln(C_{exp})$	$\tau$ (ps)
A	1.047	68	24	1.429	462	-20.45	800
B	1.151	51	48	1.431	358	-18.15	700
C	1.248	36	28	1.432	261	-16.10	600
D	1.342	26	15	1.446	167	-13.65	550

meV (C), and 167 meV (D), with GS emission at 1.151, 1.248, and 1.342 eV at 10 K.

PL spectra were obtained using a He-Ne laser (or Ar<sup>+</sup> laser for high powers) for excitation above the barrier, and recorded with a 0.5-m grating monochromator and cooled Ge diode using standard lock-in techniques. The samples were placed in a closed cycle cryostat where the temperature was varied between 10 K and 330 K. In order to study the very low excitation density regime, the beam was not focused and had a diameter of around 1 mm at the sample surface. In this way, the collected intensity remains reasonable even though the density of excitation is much smaller than that conventionally employed using a focusing lens. For an incident laser power of 4 mW and a beam size of 1 mm<sup>2</sup>, the excitation density is then only 0.5 W cm<sup>-2</sup>. Under these conditions, the PL signal is as intense as if a focusing lens was used, but the average occupation is much less than one electron-hole pair per dot. To give a more precise idea, first excited-state emission appears for values of the order of 4 W cm<sup>-2</sup>. Filters were used to further decrease the excitation when required.

### III. TEMPERATURE DEPENDENCE OF THE INTEGRATED PL INTENSITY

#### A. Experimental results

Figure 2 shows the Arrhenius plots of the integrated PL intensity (IPL) for the four samples. The experiments were performed with an excitation density of  $\approx 4$  W cm<sup>-2</sup> corresponding to the onset of the appearance of the first excited state. State blocking effects can therefore be considered negligible to a first approximation. The shape of these curves is typical of the temperature dependence for QD's. For each sample, three regimes can be identified.

(a) Low temperature regime: This is the temperature range where the IPL remains constant.

(b) Regime of strong thermal quenching: At high temperatures, the curves tend towards a straight line, characteristic of an exponential quenching  $\propto \exp(E_a/kT)$  due to thermal escape from the dots. We can deduce an activation energy  $E_a$  for each sample by measuring the slope.

(c) Intermediate regime: For intermediate temperatures, the IPL starts to drop but not yet exponentially (this is the elbow on the plots). Occasionally odd behavior such as kinks can be observed, for example, for sample B.

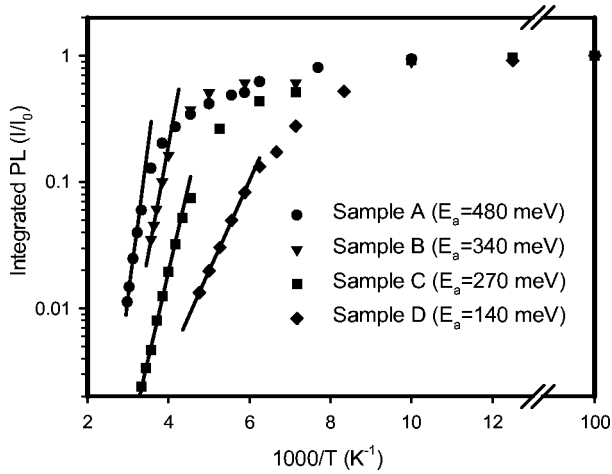


FIG. 2. Arrhenius plots of the temperature dependence of the integrated PL for sample A (circles), B (triangles), C (squares), and D (diamonds). The data have been normalized to show the same intensity at 10 K. The solid lines are linear regressions at high temperatures to extract the values of the activation energies  $E_a$ .

The exact temperature ranges of these regimes change from one sample to the other. Comparing the plots in Fig. 2, two main features can be observed.

(a) The activation energy  $E_a$  measured in the regime of strong quenching is different for each sample and matches the difference between the GaAs band gap and the ground-state energy (barrier height). This does not mean that the wetting layer (WL) is not involved in the escape as will be discussed later.

(b) The temperature at which the quenching starts increases with the barrier height (from sample D to A) approaching room temperature for 1.3- $\mu\text{m}$  emitting dots. It is, however, interesting to note that although the quenching occurs earlier for small barrier heights, it is then slower. Extrapolating the plots, the IPL of sample D should, in principle, be greater than that of C at a temperature around 340 K.

### B. Presentation of the model

In order to model the dependence of the IPL with temperature for the four samples, we describe and apply a simple model. The processes included in this model are depicted in Fig. 3. These include capture of excitons from the WL into the dots with time constant  $\tau_c$ , and escape from the dots into the WL with time constant  $\tau_e$ . The wetting layer is itself linked to the surrounding GaAs layers. Carriers can be captured from the GaAs region with a capture time  $\tau_{cw}$  and escape from the WL to the GaAs with escape time  $\tau_{ew}$ . The photogenerated carriers are assumed to be created mainly in the GaAs with a generation rate  $g$ . The carrier lifetimes in the wetting layer and GaAs are denoted as  $\tau_w$  and  $\tau_g$ , respectively, and account for radiative recombination and any other loss mechanism (e.g., nonradiative losses). Under low excitation, we can neglect state filling effects and write rate equations for  $n$ ,  $n_w$ , and  $n_g$ , the average number of carriers per dot in the QD's, the WL, and the GaAs region:

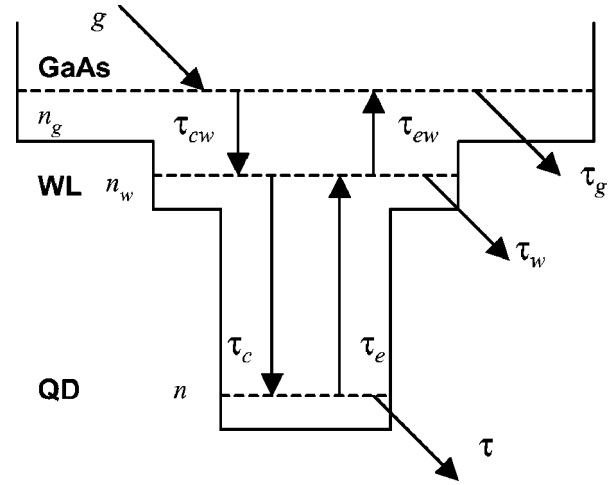


FIG. 3. Schematic of the processes taken into account in the model.

$$\frac{dn}{dt} = -\frac{n}{\tau} - \frac{n}{\tau_e} + \frac{n_w}{\tau_c},$$

$$\frac{dn_w}{dt} = -\frac{n_w}{\tau_w} - \frac{n_w}{\tau_c} - \frac{n_w}{\tau_{ew}} + \frac{n}{\tau_e} + \frac{n_g}{\tau_{cw}},$$

$$\frac{dn_g}{dt} = -\frac{n_g}{\tau_g} - \frac{n_g}{\tau_{cw}} + \frac{n_w}{\tau_{ew}} + g. \quad (1)$$

Solving the stationary state of the coupled rate equations, we obtain the integrated PL intensity from the QD's:

$$I = n/\tau = g \left[ \left( 1 + \frac{\tau_{cw}}{\tau_g} \right) \left( 1 + \frac{\tau_c}{\tau_w} + \frac{\tau}{\tau_w} R \right) + \frac{\tau_c}{\tau_g} R_w + \frac{\tau}{\tau_g} R_w R \right]^{-1}, \quad (2)$$

$$\text{where } R_w = \frac{\tau_{cw}}{\tau_{ew}} \text{ and } R = \frac{\tau_c}{\tau_e}. \quad (3)$$

In this model, all the dots are assumed to be identical and to have the same properties. The thermal redistribution of carriers cannot therefore be studied in this framework, although it would be possible to modify the rate equations to take them into account in a way similar to that described in Ref. 8. The samples studied here have relatively small FWHM and we therefore expect the redistribution effects to be negligible. This is supported by the fact that the FWHM of the PL peak is measured to be constant within the experimental errors ( $\pm 1$  meV) from 10 K to room temperature for all the samples.

Another assumption is that carriers are considered to behave as excitons or correlated electron-hole pairs. This is a common feature of most existing models,<sup>6,8,14</sup> but it will be shown in Sec. IV that this assumption is wrong and that the possible independent behavior of electrons and holes has to be taken into account. We can indeed notice in Eq. (2) that  $I$  is linearly dependent on  $g$  at all temperatures, which is com-

mon to most available models in the literature, but is in contradiction with the observations presented later in Sec. IV. Although it would be possible to generalize the rate equations to take into account the independent behavior of electrons and holes, the model would then become more complicated with many more unknown parameters. Moreover, under certain conditions, the rate equations for electrons or holes are similar to those obtained for excitons. It is therefore interesting to discuss first the model for excitons, bearing in mind that it will have to be corrected to account for the independent behavior of electrons and holes when excitation density dependence is considered. These modifications and their consequences will be discussed in Sec. IV.

This model is probably one of the simplest that one can use to describe the temperature dependence of the intensity and the exchanges between the QD's, the WL and the GaAs. However, many of the parameters can vary with temperature and we will now discuss these variations.

(a) The radiative lifetime in the dots  $\tau$  is assumed to be constant with  $T$ , as expected theoretically since carriers are confined in all three dimensions. The value of  $\tau$  has been measured at 10 K for these samples using time-resolved PL<sup>15</sup> and is between 500 and 800 ps (see Table I).

(b)  $\tau_w$  and  $\tau_g$  are the lifetimes in the WL and GaAs. They are a combination of radiative and nonradiative processes. The radiative recombination rate is expected to be of the order of 400 ps<sup>-1</sup> at low temperature and should decrease with temperature. It is therefore likely to become negligible compared to the rate of nonradiative losses at relatively low temperatures (say 50–100 K) and above.<sup>16</sup> The rate of nonradiative losses in the WL and GaAs will depend on the quality of the material. With increasing temperature, a temperature dependence similar to that reported in Ref. 16 for quantum wells can be expected, where the rate should increase and saturate around 150 K at a constant value in the range (100–1000 ps)<sup>-1</sup> depending on the quality of the material and interfaces.

(c)  $\tau_c$  and  $\tau_{cw}$  are, respectively, the capture times from the WL into the dots and from the GaAs into the WL. At 10 K, these capture times have been measured to be fast, of the order of 10 ps or less. Several authors in Refs. 17–22 have measured the temperature dependence of the rise time of the ground-state PL intensity in time-resolved experiments on QD's. Most of them have shown that the capture time from the WL into the dots decreases with temperature.<sup>17,18,21,22</sup> It was also concluded that multiphonon processes were the dominant capture mechanism at low excitations. Under higher excitations, Auger processes can become dominant at low temperatures and this will increase further the capture rate.<sup>17,21,22</sup> This is not the case at higher temperatures where the capture rate was shown to be independent of excitation except for very high excitations (much higher than those used in this work).<sup>22</sup>

(d)  $\tau_e$  and  $\tau_{ew}$  are the corresponding escape times. At 10 K, the escape rates are extremely low and increase with temperature as carriers are thermally activated outside the confining potential. It is interesting to note that in Eq. (2), the escape rates appear only in the ratios  $R$  and  $R_w$  of capture time over escape time.

From this discussion, we first see that the ratios  $\tau_{cw}/\tau_g$  and  $\tau_c/\tau_w$  should be much smaller than 1 at all temperatures, leading to a simplified expression for  $I$ ,

$$I = g \left[ 1 + \frac{\tau}{\tau_w} R + \frac{\tau_c}{\tau_g} R_w + \frac{\tau}{\tau_g} R_w R \right]^{-1}. \quad (4)$$

Since we have  $R \approx R_w \approx 0$  at low temperature, the intensity is then  $I_0 \approx g$ . Moreover,  $I$  should remain constant until one of the three factors containing  $R$  or  $R_w$  in Eq. (4) becomes of the order of 1. This is in agreement with the experiments, where a constant PL intensity is observed in the low-temperature regime.

It is important that the GaAs region is properly delimited, which is the case here owing to the AlAs/GaAs superlattices on either side of the QD layer. In this way, the photocarriers captured or escaping from the dots are confined to a GaAs region whose thickness (here 30 nm) is much smaller than the carrier diffusion length. If this is not the case, diffusion of carriers in the GaAs region should be taken into account. The main consequence is that the generation rate  $g$  would then depend on the diffusion length which would itself be dependent on the quality of the GaAs grown on either side of the dots and possibly on the quality of the surface. Since the diffusion processes and the loss mechanisms are temperature dependent, this would imply that even under a constant incoming laser power,  $g$  could vary with temperature. The interpretation of the results would then be more complicated.

### C. Escape mechanisms and activation energies

We have measured the temperature dependence of  $I/I_0$  for each sample (see Fig. 2). According to Eq. (4), this dependence should, in principle, be explained by the temperature dependence of the three factors:  $(\tau/\tau_w)R$ ,  $(\tau_c/\tau_g)R_w$ , and  $(\tau/\tau_g)R_w R$ .  $R$  and  $R_w$  are related to the escape of carriers from the dots and the WL. These ratios actually represent the balance between capture and escape between the dots and the WL (for  $R$ ) and the WL and the GaAs (for  $R_w$ ). As the temperature increases, the escape processes are thermally activated and  $R$  and  $R_w$  increase. It is often assumed that the escape rate  $\tau_e^{-1}$  is of the form

$$\tau_e^{-1} \propto e^{-E_a/kT}, \quad (5)$$

where  $E_a$  is the activation energy that has to be gained in the escape process. This leads to

$$R \propto \tau_c e^{-(E_{WL} - E_{QD})/(kT)},$$

and

$$R_w \propto \tau_{cw} e^{-(E_{GaAs} - E_{WL})/(kT)}. \quad (6)$$

We observe experimentally that for a high enough temperature the intensity exhibits an exponential quenching of the form  $I = C_{\text{exp}} e^{E_{\text{exp}}/kT}$ , where the measured activation energy  $E_{\text{exp}}$  is comparable to  $E_b = E_{\text{GaAs}} - E_{\text{QD}}$ . From Eqs. (6) and (4), the dependence with temperature of  $R$  alone or  $R_w$  alone cannot explain this behavior and only the product  $RR_w$  can lead to the correct activation energy. More precisely, the

factor  $(\tau/\tau_g)RR_w$  must be the dominant contribution to  $I$  in Eq. (4) and for that we need to assume that  $R \gg \tau_c/\tau$ ,  $R_w \gg \tau_g/\tau_w$ , and  $(\tau/\tau_g)RR_w \gg 1$ . These conditions will be met provided that the temperature is high enough (and therefore  $R$  and  $R_w$  large enough). The intensity is then given in the regime of strong quenching by

$$I \approx I_0 \frac{\tau_g}{\tau} (RR_w)^{-1}, \quad (7)$$

which combined with Eq. (6) leads to the correct dependence for  $I$ , if  $\tau_g$ ,  $\tau_{cw}$ , and  $\tau_c$  are constant with temperature. However, we already mentioned that the capture rates are likely to increase with temperature if capture is mediated by phonons. We here suggest an alternative way of explaining the observed dependence, which does not rely on the assumption made in Eq. (5) and which we believe is physically more acceptable.

It was shown recently that under low excitation, multiphonon-assisted capture was the dominant mechanism, and the capture rate from the WL to the QD's is then given by<sup>21,22</sup>

$$\tau_c^{-1} = c_0 [1 + N_{LO}(T)]^{n_d} [1 + N_{LA}(T)]^{p_d}, \quad (8)$$

where  $N_{LO}(T)$  and  $N_{LA}(T)$  are the Bose-Einstein distributions for LO and LA phonons,  $n_d$  and  $p_d$  are the number of LO and LA phonons required in the process. The difference in energy between the WL and the dot ground state is therefore  $E_{WL} - E_{QD} = n_d \hbar \omega_{LO} + p_d \hbar \omega_{LA}$ . Here, we do not consider the details of the capture mechanisms (for example, through a cascade relaxation from excited levels), but only the temperature dependence of the complete process. From Eq. (8), we see that the capture rate is temperature dependent (it increases with  $T$ ), as expected physically and as shown experimentally.<sup>17,18,21,22</sup> The contribution from spontaneous [factor 1 in Eq. (8)] and stimulated emission of phonons [factor  $N_{LO}(T)$ ] are also clearly identified. Following this argument the escape rate, due to phonon absorption, should be given by

$$\tau_e^{-1} = e_0 (N_{LO}(T))^{n_d} [N_{LA}(T)]^{p_d}. \quad (9)$$

This dependence is different from the one usually assumed [Eq. (5)]. However, taking the ratio between escape and capture rate, we can justify the exponential quenching observed experimentally:

$$R^{-1} = \frac{c_0}{e_0} e^{(n_d \hbar \omega_{LO} + p_d \hbar \omega_{LA})/(kT)} = \frac{c_0}{e_0} e^{(E_{WL} - E_{QD})/(kT)}. \quad (10)$$

The same considerations can be applied to the capture and escape processes between the WL and the GaAs leading to

$$R_w^{-1} = \frac{c_{w0}}{e_{w0}} e^{(E_{GaAs} - E_{WL})/(kT)}. \quad (11)$$

We then obtain the following expression for  $I$  in the regime of strong quenching:

$$\frac{I}{I_0} \approx \frac{\tau_g}{\tau} \frac{c_0}{e_0} \frac{c_{w0}}{e_{w0}} e^{(E_{GaAs} - E_{QD})/(kT)}. \quad (12)$$

The activation energy in this expression is the same as that obtained previously and the same as that measured experimentally. However, the previous arguments show that the factor  $\exp[E_a/(kT)]$  observed at high temperatures does not come from the temperature dependence of the escape rate alone as usually assumed [Eq. (5)] but from the dependence of the *ratio between capture and escape rates* [Eq. (10)]. At low  $T$ , only capture takes place through spontaneous emission of phonons. At high  $T$ , the stimulated emission and absorption of phonons becomes important, leading to an increase in both capture and escape rates, the latter increasing faster which results in the exponential dependence of their ratio [Eq. (10)].

Moreover, this new interpretation allows us to give a physical meaning to the coefficient in front of the exponential. We measured the values of this coefficient  $C_{\text{exp}}$  for the Arrhenius plots of each sample shown in Fig. 2. The value of  $C_{\text{exp}}$  we can extract is quite sensitive to the measured activation energy  $E_{\text{exp}}$ . Indeed, a difference of 10 meV in the measured value of  $E_{\text{exp}}$  leads to a change in  $C_{\text{exp}}$  by a factor of around  $\exp[(10 \text{ meV})/(kT)] \approx 1.5$ . To avoid any error in the measurement of  $E_{\text{exp}}$ , we used the theoretical value of  $E_{\text{exp}} = E_b = E_{\text{GaAs}} - E_{\text{QD}}$  which can be measured accurately. The value of  $C_{\text{exp}}$  is then extracted easily from a linear fit to the data in the regime of strong thermal quenching. The values obtained are summarized in Table I.  $C_{\text{exp}}$  clearly increases as we go from sample A to D. From Eq. (12), we predict that

$$C_{\text{exp}} = \frac{\tau_g}{\tau} \frac{c_0}{e_0} \frac{c_{w0}}{e_{w0}}. \quad (13)$$

In QD's, the radiative lifetime  $\tau$  is predicted to be temperature independent.  $\tau$  was measured for our samples (see Table I) using time-resolved photoluminescence<sup>15</sup> at 10 K and is assumed constant with  $T$ .  $\tau$  decreases with annealing temperature (from sample A to D) and this decrease would imply a small increase of  $C_{\text{exp}}$ . However, the change is much too small to explain the observed variation of  $C_{\text{exp}}$ , but we can take it into account by now comparing the values of  $C' = \tau C_{\text{exp}}$ . We then have  $C' = \tau_g R_0^{-1} R_w^{-1}$ , where  $R_0$  is the ratio,  $R_0 = e_0/c_0$  and  $R_w = e_{w0}/c_{w0}$ .

$\tau_g$  is the lifetime in the GaAs and can be assumed constant with temperature above 150 K. Because all the samples were derived from the same wafer, the quality of the samples should be similar. The anneals could, in principle, have passivated some defects resulting in a smaller value of  $\tau_g$  for sample A compared to the annealed samples. However, such an improvement is usually observed only in samples where defects have been deliberately introduced. Studies of  $\text{In}_x\text{Ga}_{1-x}\text{As}/\text{GaAs}$  quantum wells have actually shown that annealing had no effect on the PL intensities.<sup>23</sup> Moreover, any improvements would be of a similar magnitude for samples B, C, and D, for which the annealing temperature is similar. For these samples, the value of  $C'$  changes continu-

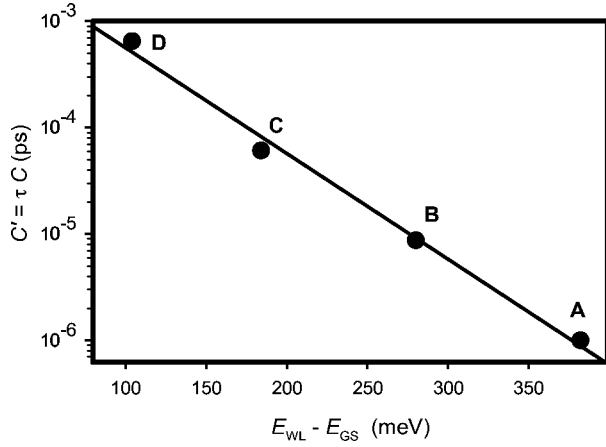


FIG. 4. Variation of  $C' = \tau C_{\text{exp}}$  across our samples on a log scale, as a function of the energy difference between the WL and the QD's,  $E_{\text{WL}} - E_{\text{QD}}$ . The dependence is nearly linear.

ously over two orders of magnitude, and a change in  $\tau_g$  of this order as a result of annealing is highly unlikely. There must therefore be another mechanism, which can then explain the variation of  $C'$  from sample A to B, without invoking a change in  $\tau_g$ . We will therefore assume that  $\tau_g$  is the same for the four samples and constant with  $T$  above 150 K, where the measurements of  $C_{\text{exp}}$  are performed.

Similarly, the WL emission does not change very much upon annealing (see Table I). We can therefore assume that  $R_{w0}$  does not vary too much across the samples. We conclude that the large variation of  $C_{\text{exp}}$  across the samples must be due to a variation of  $R_0 = e_0/c_0$ , where  $c_0$  and  $e_0$  were defined previously when characterizing the capture and escape rates, and are related to emission and absorption of phonons. For photons, stimulated emission and absorption rates are usually identical for a given transition and the calculation of these rates usually relies on the application of Fermi's golden rule. For absorption and emission of phonons, the calculations would be more complicated,<sup>24</sup> but similar. The important point is the density of final states, which also appears in the calculation. This means that if the upper state has a degeneracy twice as large as the lower state, then the rate of absorption (corresponding to escape in our case) will be twice as large as the rate of stimulated emission (corresponding to capture). The ratio  $R_0$ , and also  $C'$  are therefore a reflection of the decreased degeneracies of the states when going from the barrier to the ground state of the dots.

To understand and quantify the variation of  $C'$  across our samples, we plotted in Fig. 4  $\ln(C')$  as a function of the energy difference between the WL and the QD's,  $E_{\text{WL}} - E_{\text{QD}}$ . The plot obtained is a straight line meaning that  $C' \propto \exp[-(E_{\text{WL}} - E_{\text{QD}})/E_m]$  with  $E_m \approx 44$  meV. Probably a more meaningful way to write this dependence is

$$C' = a2^{-(E_{\text{WL}} - E_{\text{QD}})/\hbar\omega_{\text{LO}}} \approx \frac{a}{2^{n_d}}, \quad (14)$$

where  $n_d$  is the total number of LO phonons involved in the complete capture process from the WL to the GS of the dots. We can also extract  $a \approx 0.005$  ps. From the measured values

of  $E_m$ , the corresponding value of  $\hbar\omega_{\text{LO}}$  is  $E_m \ln(2) \approx 30.5$  meV. This value is in good agreement with the LO phonon energy in InAs (30 meV). From Eqs. (13) and (14), we deduce that

$$R_0 \propto 2^{n_d}. \quad (15)$$

This dependence suggests that capture and escape of carriers proceeds, at least at high temperatures, through a cascaded emission and absorption of LO phonons. Moreover, for each LO phonon involved in the capture or escape, a factor of 2 appears in the ratio between escape rate and capture rate. This might seem surprising at first, since one could have instead expected a factor of 2 to appear for each excited state of the dot due to the increase in degeneracy. However, there is increasing evidence that for QD's, excitons and phonons are in a strong-coupling regime leading to the formation of polarons.<sup>25-27</sup> The energy levels of polarons can be very different from that of noninteracting particles in the dots<sup>26,27</sup> and can play an important role in the capture, relaxation, and escape of carriers.<sup>28</sup> This can, for example, lead to the presence of an additional electronic state with a fourfold degeneracy including spin, at around 30 meV above the ground state. The presence of such a state was recently shown to be required to interpret the temperature dependence of far-infrared absorption in QD's.<sup>29</sup> The presence of a similar ladder of states spaced by  $\approx 30$  meV with increasing degeneracies in the polaron energy levels could explain the origin of the factor  $2^{n_d}$  we measure. Such speculations would need to be investigated with a complete calculation of the polaron states and of their decay rates.

The one-particle model presented so far has been shown to yield some interesting insights into the temperature dependence of QD's. However, we will now present experimental results that clearly show that such models have limits and that the independent behavior of electrons and holes needs to be taken into account when the excitation density dependence is considered.

#### IV. SUPERLINEAR DEPENDENCE OF THE IPL WITH EXCITATION

The effects presented so far had already been reported for conventional as-grown samples. However, there have not been many studies of the excitation dependence of the IPL at different temperatures.<sup>30</sup> In the following, we present the results of such experiments, where a *strong superlinearity is observed at high temperatures*. The experiments have been carried out on all four samples and similar results were obtained for all of them. For the as-grown sample, the barrier is so high that the regime of strong thermal escape (or strong quenching) is not really reached at 300 K. We will therefore present mainly the results obtained for sample C, where we can more easily probe the strong thermal quenching regime.

##### A. Experimental results

Figure 5 shows the Arrhenius plots of the IPL between 100 K and 300 K for different excitation densities. The largest excitation density is estimated to be  $4 \text{ W cm}^{-2}$  and cor-

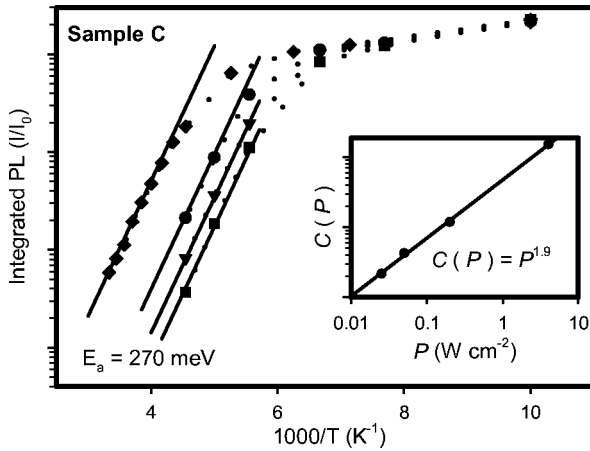


FIG. 5. Arrhenius plots of the temperature dependence of the IPL from sample C between 100 K and 300 K, at different excitation densities:  $4 \text{ W cm}^{-2}$  (diamonds),  $0.2 \text{ W cm}^{-2}$  (circles),  $50 \text{ mW cm}^{-2}$  (triangles), and  $25 \text{ mW cm}^{-2}$  (squares). The curves have been normalized to show the same intensity at 10 K. The divergence of these curves reflects how the ratio between the intensities changes with temperature. Solid lines are linear regressions at high temperatures to extract the values of the activation energies  $E_a$  and of the coefficient of the exponential  $C$ . Dotted lines are a guide for the eye. The inset shows the log-log plot of  $C$  as a function of power  $P$ . The linear regression indicates a nearly quadratic law.

responds to the intensity for which we start seeing a small signal from the first excited state. The three other sets of data were obtained with excitation densities 20, 80, and 160 times smaller. The data have been normalized to have the same IPL at 10 K. The IPL remains constant between 10 K and 100 K for the four cases (not shown here). The shape of these plots is typical of the temperature dependence for QD's with an exponential quenching at high temperatures (see Sec. III). Measuring the slope at high temperatures gives us the activation energy for thermal escape from the dots. These activation energies are equal in all four cases within the experimental errors. We derive a value of  $E_a \approx 270 \text{ meV}$ , which matches the barrier height of this sample. It is not surprising to find the same activation energy in the four cases as the barrier height should not be dependent on the excitation density. However, as the excitation level decreases, the quenching of the IPL occurs at smaller temperatures. We clearly see in Fig. 5 that the curves diverge as the temperature increases. If, at each given temperature, the dependence upon excitation density was linear, the four curves should be indistinguishable. This is the case between 10 K and 150 K, but for higher temperatures where thermal escape becomes dominant, the divergence of these curves shows that the dependence becomes superlinear. A similar behavior was observed in Ref. 9 above room temperature and attributed without justification to saturation of the losses in the barrier.

To investigate this further, we made a more comprehensive study of the excitation density dependence of the IPL in the temperature range from 10 K to 220 K. The excitation density was decreased from 500 to only  $16 \text{ mW cm}^{-2}$ , giving a range of nearly two orders of magnitude. Note that all these excitation densities are in the regime where the number

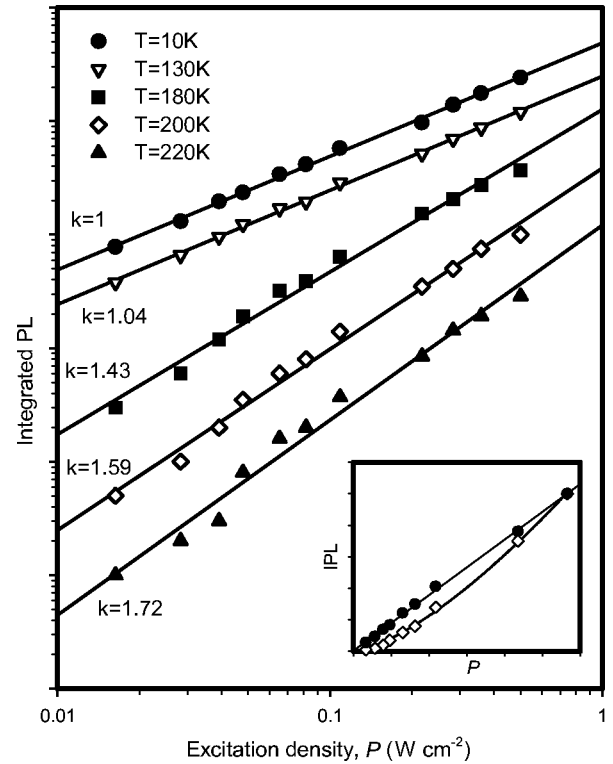


FIG. 6. Log-log plot of the excitation density versus the integrated photoluminescence at different temperatures for sample C. The solid lines are linear regressions. A slope of  $k=1$  ( $T=10 \text{ K}$  and  $130 \text{ K}$ ) reflects a linear dependence. Slopes larger than 1 represent a superlinear dependence. The inset shows the same plot on a linear scale for  $T=10 \text{ K}$  and  $T=200 \text{ K}$ , where the superlinear dependence is clearly seen for the higher temperature.

of electron-hole pairs per dot is much smaller than 1 and we do not see any emission from the excited states at 10 K. To highlight the nonlinearities, the excitation density can be plotted against the IPL in a log-log plot at different temperatures. Figure 6 shows the results obtained at 10 K, 130 K, 180 K, 200 K, and 220 K. The straight lines are linear regressions. A purely linear behavior is characterized by a slope of exactly 1 and is what we observe for temperatures smaller than 150 K. However, at higher temperatures, the slope increases, being close to 1.7 at 220 K. The behavior is then superlinear, as can be seen more clearly on a linear plot shown in the inset of Fig. 6.

Given the fact that the activation energy of the thermal escape is not dependent on the excitation level, the curves in Fig. 5 tend, at high temperatures, towards parallel straight lines. In this regime, we should therefore find a fixed law for the excitation dependence of the IPL at all higher temperatures. However, it is difficult to give a definite conclusion on this issue, because the intensity is then three to four orders of magnitude lower than those measured in conventional experiments, and the errors begin to be significant. An easier way to extract this law is to use the linear regressions obtained in Fig. 5. In this regime, the intensity is  $I(P, T)/I_0 = C(P)\exp[E_a/(kT)]$ . Since  $E_a$  is the same at all powers, the power dependence of  $I$  at a fixed high temperature is governed by  $C(P)$ . In the inset of Fig. 5, we plot the measured

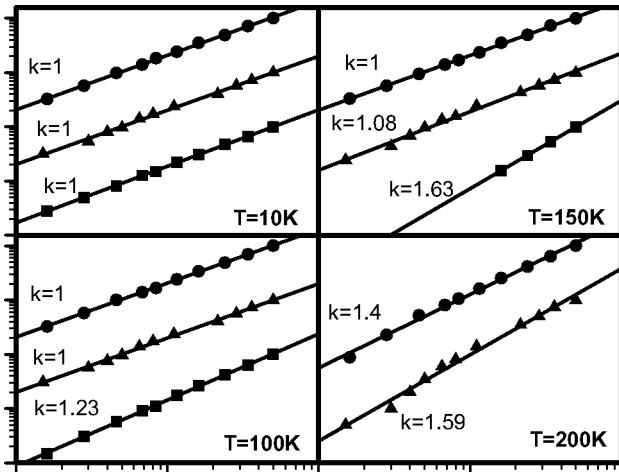


FIG. 7. Log-log plot of the excitation density versus the integrated photoluminescence at different temperatures for samples *B* (circles), *C* (triangles), and *D* (squares). The solid lines are linear regressions and the degree of superlinearity is indicated by a measure of the slopes  $k$ . The superlinearity appears at lower temperatures as we move from sample *B* to *D*.

values of  $\ln[C(P)]$  for each of the four plots of Fig. 5 as a function of  $\ln(P)$ . The plot is linear with a slope of 1.9. Given the experimental errors, it is reasonable to assume that the slope is close to 2, leading to a quadratic dependence of the intensity with power at a fixed temperature in the regime of strong quenching:  $I(P) \propto C(P) \propto P^2$ .

Similar results were obtained for all the other samples. The only difference is the temperature for which these effects appear. Figure 7 compares the superlinearity of samples *B*, *C*, and *D* at different temperatures. We see that the superlinearity occurs at lower temperatures for samples with a lower barrier height. For all of them, the appearance of the superlinearity actually coincides with the characteristic temperature for which the IPL starts dropping (intermediate regime). This is a very important observation, because it shows that this effect is directly related to the thermal escape of carriers in the barrier material. Another important point is that this effect is not dependent on the energy of the carriers in the barrier. Similar results were obtained with a He-Ne laser (excitation at 1.96 eV) and an Ar<sup>+</sup> laser (at 2.41 eV). This effect was also observed on a large number of other as-grown InAs/GaAs QD samples, and we therefore believe it is quite general.

Finally, all the previous experiments were performed at low or very low excitation density, where little excited-state emission is observed. The number of  $e-h$  pairs per dot was therefore smaller or much smaller than 1. It is interesting to study what happens at higher excitations. Figure 8 shows such a study on a sample similar to *A*. This experiment was performed at 293 K, which is in the regime of strong quenching. The highest excitation was  $120 \text{ W cm}^{-2}$ , which corresponds roughly to eight  $e-h$  per dot, and the lowest was 100 times smaller, where there is much less than one  $e-h$  pair per dot. The superlinear behavior is again observed in the regime of low excitation with a dependence close to quadratic (slope of 2 on a log-log plot). However, this superlinearity becomes

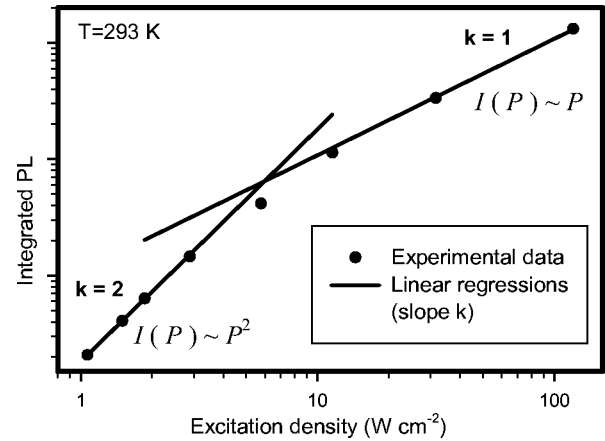


FIG. 8. Log-log plot of the integrated photoluminescence as a function of excitation density at 293 K (symbols). The solid lines are linear regressions with slopes  $k=2$  (low power) and  $k=1$  (high power). The dependence is therefore close to quadratic at low excitations but becomes linear at high excitations.

weaker as the power increases and approaches linearity (slope of 1) at the highest power. The change from quadratic to linear occurs over a range of excitation density corresponding to 6–7 dB (a multiplying factor of 4–5). Interestingly, this change coincides with an increase in the emission from the first excited state. This indicates that it is related to the fact that the average number of  $e-h$  pairs per dot changes from smaller than 1 to larger than 1. This observation is very important for the interpretation of the origin of the superlinear behavior.

## B. Possible explanations

We believe that the superlinearity we observe is quite general to QD samples. However, all the models available in the literature assume a linear dependence with excitation and cannot explain this behavior. Because it is especially important at room temperature, where most devices operate, it is of great interest for applications to understand the mechanisms responsible. The experimental results show that the superlinearity becomes important at a temperature which is dependent on the sample studied. More specifically, its appearance is correlated with the escape of carriers from the dots into the barrier (and hence the quenching of the intensity). The superlinearity is stronger as the temperature increases or as the excitation density decreases. In the regime of strong quenching, the superlinear behavior tends towards a quadratic law. Finally, if the excitation density is sufficiently increased to a level where there is one  $e-h$  pair or more per dot on an average, the dependence then comes back to linear.

We will now consider three mechanisms that could explain this phenomenon, and show that only the third one is fully compatible with the set of experimental results.

(a) The first mechanism that can be invoked to explain a superlinear dependence of the intensity is a possible saturation of the losses.<sup>9</sup> If part of the losses in the barrier material or WL can be saturated when the population in the barrier increases, a superlinear dependence would be observed, but

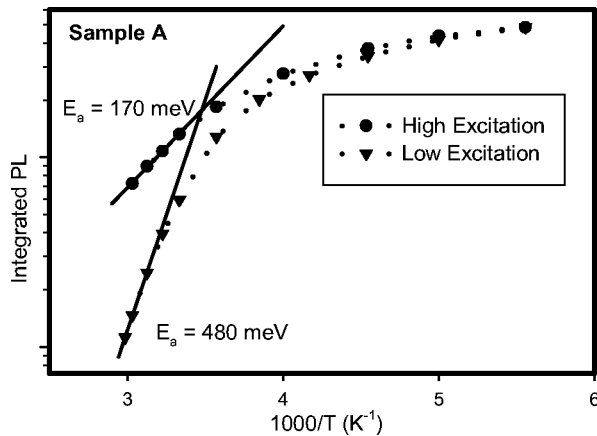


FIG. 9. Arrhenius plots between 180 K and 330 K of sample A at low ( $4 \text{ W/cm}^2$ ) and high ( $100 \text{ W/cm}^2$ ) excitations. Solid lines are linear regressions at high temperatures. The activation energy is much smaller at high excitation where the power dependence is also linear instead of quadratic.

only when the population in the barrier is sufficient to saturate the losses, i.e., when escape from the dot becomes important, which is compatible with the observation. However, a decrease of the power should result in a decrease of the population in the barrier so that saturation effects would become negligible. Similarly, an increase of the power would result in a complete saturation of the losses and the dependence would return to linear. At a given temperature where carrier escape is not negligible, the superlinearity should therefore be observed only for intermediate excitations, while a linear dependence would be observed for the lowest and highest excitations, in contradiction with our observations at very low excitation. There is a possibility that the linear regime would only be reached for excitations lower than used here, which might explain why we do not observe it. However, the superlinear regime should only extend over a limited range of excitation where losses are partially saturated. This is incompatible with the results presented in the inset of Fig. 5, where a quadratic dependence is observed over nearly two orders of magnitude. Moreover, the saturation of losses should result in a varying degree of superlinearity and not a quadratic dependence as observed. We conclude that this phenomenon of saturation of losses in the barrier, if present, does not play a dominant role in the superlinearity observed here. A further confirmation of this conclusion can be gained from the results presented in Fig. 9 and discussed in Sec. IV C: the observation of two distinct activation energies at low and high excitations cannot be understood if saturation of losses is the only mechanism responsible for the superlinearity.

(b) Another source of superlinearity could be the possibility of Auger processes in the capture of carriers into the dots.<sup>31</sup> Although Auger-assisted capture is thought to be negligible at low temperatures and low excitations, an Auger mechanism involving carriers in the barrier could become dominant over other phonon-assisted capture processes at higher temperatures when many carriers escape from the dots and end up in the barrier material. In this regime, the capture rate would become proportional to the excitation density, and

this would lead to a quadratic dependence of the PL with excitation. However, as the excitation density increases further, Auger-assisted capture should become more and more dominant and the quadratic dependence should be even more prominent. Also, if the excitation density is decreased sufficiently, Auger processes should eventually become negligible and a linear dependence should be observed. This is in opposition with our observations, showing that the dependence becomes linear when the power is increased and quadratic at low excitations. We conclude that Auger-assisted capture cannot be the dominant capture mechanism in the conditions where superlinearity is observed. This is in agreement with measurements showing that phonon-assisted processes are dominant at room temperature even under high excitations.<sup>22</sup> Auger processes cannot therefore be responsible for the superlinear effects we observe.

(c) The final explanation we propose assumes that electrons and holes can be captured and can escape independently, at least in the regime where superlinearity is observed. If this is the case, then electrons and holes are captured randomly by the dots, and possibly by different dots. At low excitation when much less than one  $e-h$  pair is available per dot on average, the probability that one electron and one hole are captured in the same dot depends quadratically upon power, explaining the superlinearity. Moreover, as the average occupation becomes close or higher than one  $e-h$  pair per dot, this probability will then vary linearly with power, in agreement with the observation. This assumption is therefore the most probable explanation of our results and will now be discussed in more detail and shown to agree qualitatively with all the experimental results.

### C. Independent capture of electrons and holes

In many studies and models of the temperature dependence of QD's, only one type of carrier (or one particle) is considered. This is justified if the electrons and holes remain bound as excitons in both the dots and the barrier at all temperatures or if they behave as correlated electron-hole pairs. However, given that the typical exciton binding energies either in bulk or QW's are believed to be  $\approx 10 \text{ meV}$  at most, this assumption is unlikely to be correct at high temperatures. Another justification of the one-particle approach could be that only one type of carrier can thermally escape at the temperatures investigated, while the other remains in the dots. However, if this were the case, the activation energy measured in the regime of strong quenching should match the barrier height of the escaping carrier only and not the total barrier height. Similarly, if carriers behaved as correlated electron-hole pairs, the measured activation energy should be half of the total barrier height.<sup>14</sup> This is in contradiction with our previous measurements showing that the activation energy is in fact equal to the sum of the barrier height for electrons *and* holes. We conclude that, at high temperatures, both electrons and holes escape from the dots and that they do not behave as correlated pairs.

Another indication that electrons and holes can escape independently can be inferred from photocurrent (PC) experiments, although one has to bear in mind that the electric

fields used in such experiments could affect the electron/hole behaviors compared to PL. It was shown in Ref. 32 that the activation energy of the PC signal corresponds to the barrier height of the less confined carriers. This activation energy was measured to be  $\approx 30\%$  of the total barrier height and was attributed to the hole barrier height. This confirms that the electrons and holes can escape separately and these measurements should also, in principle, tell us which type of carrier escapes first. However, we can interpret the results in two ways: In PC measurements, carriers are created directly inside the dots and give rise to a current if they are able to escape. If only one type of carrier escapes, one could argue that light absorption is then prevented by the presence of the remaining carriers in the dot, and the PC signal remains small until the second type of carrier escapes (at higher temperatures). With this interpretation, the measured activation energy should correspond to that of the more slowly escaping carriers. However, it is also possible to argue that when one type of carrier escapes, an electric field should build up, which is then strong enough to assist the escape of the other type of carrier. In this case, the activation energy of the process would be that of the fast escaping carriers. This issue therefore requires further experiments before a definitive conclusion is reached.

We will now show that the assumption of independent escape of electrons and holes is compatible with the PL experiments presented earlier, and that it provides an explanation for the superlinearity. The superlinearity can, in principle, be observed if electrons and holes can be captured independently in different dots *and* if there is a loss mechanism in addition to the radiative emission of an  $e$ - $h$  pair in a dot.

First, in the low-temperature regime, the power dependence of the intensity is always linear (except at very high excitation where state blocking effects are important leading to a saturation not considered here). There are two possible explanations for this linearity. If electrons and holes are captured into the dots as pairs or excitons at low temperatures, this would simply explain the linearity (see, for example, Sec. III). However, even if electrons and holes were captured independently in different dots, a linear dependence would also be observed when escape times are long (which is the case at low temperatures) and if nonradiative recombination is negligible when only an electron or a hole occupies the ground state of a dot. In this case, under cw excitation, charged QD's would always eventually capture a carrier of the opposite charge and emit a photon. The PL intensity would then be  $I=g$  as is the case for excitonic capture. This scenario is also supported by PL experiments on single dots, which usually show emission from charged excitons<sup>33,34</sup> implying that electrons and holes can be captured independently even at low temperatures. Another way to confirm this would be to study the power dependence (under low excitation) of the integrated PL intensity for pulsed excitation (with various delays between pulses). A linear dependence would mean that exciton capture is dominant, while a quadratic dependence would point towards a fully independent capture of charge carriers. For the present study, both interpretations are compatible with experiments.

As the temperature increases, the carriers captured in the dots will start to escape into the barrier where they can be lost nonradiatively, leading to a drop in the IPL (intermediate regime). If carriers escaped as excitons or pairs and could be recaptured as excitons or pairs, the power dependence of the IPL in this case would be linear (see Sec. III). In fact, we have shown that the drop in PL intensity correlated with the appearance of the superlinearity (which is a sign of independent behavior of electrons and holes). This implies that even if carriers are captured as excitons or pairs, they escape independently from the dots and can then be recaptured randomly. There is, therefore, a probability that they are not recaptured by a dot already containing a carrier of the other type, especially at low excitations. This leads to the appearance of the superlinear dependence.

It is, in principle, possible that in the regime of strong quenching, the second type of carrier still does not escape from the dots. However, if this was the case, the activation energy measured in this regime should be equal to the barrier height of the escaping carriers only. This is in contradiction with the measurements of the activation energy, which matches the total barrier height (electrons + holes). We conclude that both types of carrier escape from the dots in the regime of strong quenching.

In this regime, capture and escape of electrons and holes into and outside the QD's becomes completely uncorrelated. The model presented in Sec. III for excitons could be applied in a first approximation independently to both electrons and holes. The problem of this approximation is that it can lead to an imbalance between the total electron and hole populations in the crystal. To avoid this, one has to modify the terms corresponding to losses or radiative recombination so that they are symmetrical for electrons and holes. This, however, leads to coupled rate equations, possibly nonlinear, which cannot be solved analytically. For the purpose of the argumentation here, we will therefore rely on a simple assumption valid only for the regime of strong quenching to extract qualitative results. The development and resolution of a comprehensive model taking into account the uncorrelated dynamics of electrons and holes is important but is outside the scope of this paper. We assume that the average population  $n_i$  of electrons ( $i=e$ ) or holes ( $i=h$ ) in the dots is given to a first approximation in the regime of strong quenching by

$$n_i \propto g e^{E_a^i/kT}, \quad (16)$$

where  $E_a^e$  ( $E_a^h$ ) is the barrier height for the electrons (the holes), and  $g$  is the generation rate, which is identical for both carriers. This expression is analogous to Eq. (12) obtained for excitons. It seems logical to apply it to electrons and holes independently in this regime since capture and escape of electrons and holes are uncorrelated. There can be an imbalance between electron and hole populations in the QD's, but this would be compensated by different populations of electrons and holes in the barrier, and it is therefore compatible with the neutrality of the crystal. The details of the loss mechanisms, assuring this neutrality, will only affect the coefficient of proportionality in Eq. (16).

Under low excitation ( $n_e, n_h \ll 1$ ), the probability that a given dot is occupied by both an electron and a hole is equal to  $n_e n_h$ . The PL intensity is then of the form:

$$I \propto g^2 e^{(E_a^e + E_a^h)/kT}. \quad (17)$$

We first see that within our hypotheses, the activation energy in the regime of strong quenching and at low excitations is  $E_a = E_a^e + E_a^h$ , in agreement with the observations of Sec. III and with the model for excitons. However, this expression now also predicts that the IPL should vary quadratically with excitation density at high temperatures and low excitations, as observed earlier in this section.

Moreover, as the excitation is increased,  $n_e$  and  $n_h$  both increase with  $g$ . Above a certain value of  $g$ , one of them,  $n_s$ , will reach a value comparable to 1 (where the subscript  $s$  corresponds to the more slowly escaping carrier,  $e$  or  $h$ ). At this stage, most of the dots will on average contain at least one carrier of type  $s$ . In this regime, the PL intensity will then be determined by the average occupation of the other type of carrier in the dots for which  $n_f \ll 1$  is still valid (we use subscript  $f$  for fast escape). In this case, the IPL should have the form

$$I \propto n_f \propto g e^{E_a^f/kT}. \quad (18)$$

This explains why the superlinearity disappears at high excitations, even if the temperature is high, coming back to a linear dependence of  $I$  with  $g$ . Moreover, according to this expression, we should observe in this regime a smaller activation energy  $E_a^f$  corresponding to the barrier height of the faster escaping carriers. Figure 9 shows a comparison of the Arrhenius plots of sample *A* at low and high excitations. In the regime of strong quenching (high temperatures), the power dependence is linear at high power and quadratic at low excitation as already shown. It is apparent in the figure that the activation energy is strongly reduced at high excitations, which confirm the previous arguments. This activation energy, which we measure to be  $E_a^f \approx 170$  meV, should also coincide with the barrier height of the faster escaping carrier. This has to be compared with the total barrier height of  $E_a = 462$  meV for this sample. We conclude that the carriers that escape faster are the holes (which are known to be less confined). We can also extract the value of the valence-band offset ratio:  $E_a^h/E_a \approx 37\%$ , which is in good agreement with reported values.<sup>32</sup>

These measurements therefore strongly support our hypothesis of independent escape of electrons and holes. This not only explains the origin of the superlinear behavior, but also the return to linearity at high excitations and the changes in the activation energy.

#### D. Discussion and implications

We have shown that the assumption that electrons and holes escape and are recaptured into the dots independently is consistent with the experimental results. Although it is reasonable, this assumption was never studied in detail previously. This assumption is in some respects compatible with our previous one-particle model but, moreover, enables to

understand a number of unexplained results, especially the superlinear dependence of the PL intensity with excitation. Another important consequence is that the activation energy can be strongly dependent on the excitation density, which provides an explanation for the wide range of activation energies reported in the literature for QD's. Under low excitation, it should be equal to the total barrier height of electrons and holes, while it only corresponds to the barrier height of one type of carrier (probably holes) under high excitation. Here, we defined barrier height as the energy difference between GaAs and QD ground state. However, it can be seen in Eq. (4) that in some cases, the activation energy would actually correspond to the energy difference between the WL and the ground state. This could be the case if there was a significant loss mechanism in the WL, due, for example, to poor material quality or dislocations, leading to a very small lifetime  $\tau_w$ . The term containing the ratio  $R$  would then be the dominant contribution instead of the term with  $R_w R$  as was the case in this paper. Overall, many different activation energies can be measured on similar samples depending on the excitation density and the material quality.

Although good fits to the data can be obtained using the one-particle model presented in Sec. III, it would be difficult to give a physical meaning to the parameters derived from these fits. Indeed this model is only approximate and cannot explain the power dependence. Although most conclusions obtained from this model are valid qualitatively, a generalized model taking into account the independent capture of electrons and holes is required for a comprehensive and quantitative analysis. We showed here that simple approximations could be made in the regime of strong quenching. It would be possible to generalize the rate equations of Sec. III to take into account such effects at all temperatures, but it would add more unknown parameters such as relative escape or capture rates of electrons and holes, or exciton breaking time. Moreover, the resulting rate equations would be coupled and most likely nonlinear, making an analytical resolution impossible. Despite these difficulties, such a model could confirm that many of the conclusions obtained from one-particle models, especially those not involving different excitation densities, are still valid.

The superlinear behavior could, in principle, have some impact on the understanding of some devices, such as lasers. At first, one could argue that a laser operates in a regime where the excitation density is sufficiently high to avoid the superlinear effects. However, these effects could be important in the determination of the threshold or of  $T_0$  values, for example. Moreover, if electrons and holes behave differently at room temperature, it is important to try and understand their respective roles. This could have implications in the design of devices, and particularly in the way carriers should be injected in optoelectronic devices for optimum performance. For example, it was shown recently that QD lasers with  $p$ -doped QD layers exhibit much better temperature performance than undoped layers,<sup>35</sup> which further supports our results.

Finally, it is often assumed that comparing the PL intensity of two samples is a good method of assessing their respective quality. In the light of our results, this is not so

straightforward. In fact, the ratio of the PL intensities of the two samples could change with excitation density and also with QD density (which determines the average number of carriers per dot for a given excitation density). One therefore has to be careful when assessing the quality of QD samples only through a comparison of their PL efficiencies at a given power and temperature.

## V. CONCLUSION

We have presented a set of experimental results related to the temperature dependence of the PL intensity in annealed InAs/GaAs quantum dots. An extensive study of the influence of the excitation density at different temperatures has revealed a number of experimental facts. The power dependence of the PL intensity was shown to be linear at low temperatures, but to become increasingly superlinear and

eventually quadratic as carriers are thermally activated from the QD's. When the excitation density is increased sufficiently, the power dependence returns to linear, even at high temperatures. All these results can be understood if it is assumed that electrons and holes escape and are recaptured independently. We also presented a simplified model to back these arguments. The comparison of the results across a range of annealed samples also enabled us to shed new light on the mechanisms of capture and escape at high temperatures. Phonons, or possibly polarons, were shown to play a major role in the balance between escape and capture. More work is now required to link these experimental results with theoretical calculations of phonon absorption and emission rates. We believe our arguments can explain many apparently contradictory results reported in the literature on the temperature dependence of the photoluminescence of QD's.

\*Electronic address: e.leru@ic.ac.uk

- <sup>1</sup>D.I. Lubyshev, P.P. González-Borrero, E. Marega, E. Petitprez, N. La Scala, and P. Basmaji, *Appl. Phys. Lett.* **68**, 205 (1996).
- <sup>2</sup>L. Brusaferrri, S. Sanguinetti, E. Grilli, M. Guzzi, A. Bignazzi, F. Bogani, L. Carraresi, M. Colocci, A. Bosacchi, P. Frigeri, and S. Franchi, *Appl. Phys. Lett.* **69**, 3354 (1996).
- <sup>3</sup>S. Fafard, S. Raymond, G. Wang, R. Leon, D. Leonard, S. Charbonneau, J. L. Merz, P.M. Petroff, and J.E. Bowers, *Surf. Sci.* **361**, 778 (1996).
- <sup>4</sup>Z.Y. Xu, Z.D. Lu, X.P. Yang, Z.L. Yuan, B.Z. Zheng, J.Z. Xu, W.K. Ge, Y. Wang, J. Wang, and L.L. Chang, *Phys. Rev. B* **54**, 11528 (1996).
- <sup>5</sup>K. Mukai, N. Ohtsuka, and M. Sugawara, *Appl. Phys. Lett.* **70**, 2416 (1997).
- <sup>6</sup>H. Lee, W. Yang, and P.C. Sercel, *Phys. Rev. B* **55**, 9757 (1997).
- <sup>7</sup>C. Lobo, R. Leon, S. Marcinkevičius, W. Yang, P.C. Sercel, X.Z. Liao, J. Zou, and D.J.H. Cockayne, *Phys. Rev. B* **60**, 16647 (1999).
- <sup>8</sup>S. Sanguinetti, M. Henini, M. Grassi Alessi, M. Capizzi, P. Frigeri, and S. Franchi, *Phys. Rev. B* **60**, 8276 (1999).
- <sup>9</sup>A. Patanè, A. Polimeni, P.C. Main, M. Henini, and L. Eaves, *Appl. Phys. Lett.* **75**, 814 (1999).
- <sup>10</sup>E.C. Le Ru, P.D. Siversns, and R. Murray, *Appl. Phys. Lett.* **77**, 2446 (2000).
- <sup>11</sup>R. Murray, D. Childs, S. Malik, P. Siversns, C. Roberts, J.-M. Hartmann, and P. Stavrinou, *Jpn. J. Appl. Phys., Part 1* **38**, 528 (1999).
- <sup>12</sup>R. Leon, Yong Kim, C. Jagadish, M. Gal, J. Zou, and D.J.H. Cockayne, *Appl. Phys. Lett.* **69**, 1888 (1996).
- <sup>13</sup>S. Malik, C. Roberts, R. Murray, and M. Pate, *Appl. Phys. Lett.* **71**, 1987 (1997).
- <sup>14</sup>W. Yang, R.R. Lowe-Webb, H. Lee, and P.C. Sercel, *Phys. Rev. B* **56**, 13314 (1997).
- <sup>15</sup>S. Malik, E.C. Le Ru, D. Childs, and R. Murray, *Phys. Rev. B* **63**, 155313 (2001).
- <sup>16</sup>G. Bacher, C. Hartmann, H. Schweizer, T. Held, G. Mahler, and H. Nickel, *Phys. Rev. B* **47**, 9545 (1993).
- <sup>17</sup>B. Ohnesorge, M. Albrecht, J. Oshinowo, A. Forchel, and Y. Arakawa, *Phys. Rev. B* **54**, 11532 (1996).
- <sup>18</sup>S. Marcinkevičius and R. Leon, *Phys. Rev. B* **59**, 4630 (1999).
- <sup>19</sup>L. Zhang, T.F. Boggess, D.G. Deppe, D.L. Huffaker, O.B. Shchekin, and C. Cao, *Appl. Phys. Lett.* **76**, 1222 (2000).
- <sup>20</sup>T.F. Boggess, L. Zhang, D.G. Deppe, D.L. Huffaker, and C. Cao, *Appl. Phys. Lett.* **78**, 276 (2001).
- <sup>21</sup>J. Feldmann, S.T. Cundiff, M. Arzberger, G. Böhm, and G. Abstreiter, *J. Appl. Phys.* **89**, 1180 (2001).
- <sup>22</sup>M. De Giorgi, C. Lingk, G. von Plessen, J. Feldmann, S. De Rinaldis, A. Passaseo, M. De Vittorio, R. Cingolani, and M. Lomascolo, *Appl. Phys. Lett.* **79**, 3968 (2001).
- <sup>23</sup>W.P. Gillin, D.J. Dunstan, K.P. Homewood, L.K. Howard, and B.J. Sealy, *J. Appl. Phys.* **73**, 3782 (1993).
- <sup>24</sup>T. Inoshita and H. Sakaki, *Phys. Rev. B* **56**, R4355 (1997).
- <sup>25</sup>S. Hameau, Y. Guldner, O. Verzelen, R. Ferreira, G. Bastard, J. Zeman, A. Lemaître, and J.-M. Gérard, *Phys. Rev. Lett.* **83**, 4152 (1999).
- <sup>26</sup>O. Verzelen, R. Ferreira, and G. Bastard, *Phys. Rev. B* **62**, R4809 (2000).
- <sup>27</sup>O. Verzelen, R. Ferreira, and G. Bastard, *Phys. Rev. Lett.* **88**, 146803 (2002).
- <sup>28</sup>S. Sauvage, P. Boucaud, R.P.S.M. Lobo, F. Bras, G. Fishman, R. Prazeres, F. Glotin, J.M. Ortega, and J.-M. Gérard, *Phys. Rev. Lett.* **88**, 177402 (2002).
- <sup>29</sup>F. Bras, P. Boucaud, S. Sauvage, G. Fishman, and J.-M. Gérard, *Appl. Phys. Lett.* **80**, 4620 (2002).
- <sup>30</sup>E.C. Le Ru, J. Fack, and R. Murray, in *Semiconductor Quantum Dots II*, edited by R. Leon, S. Fafard, D. Huffaker, and R. Notzel, MRS Symposia Proceedings No. 642 (Materials Research Society Pittsburg, 2001), p. 28.1.
- <sup>31</sup>S. Raymond, K. Hinzer, S. Fafard, and J.L. Merz, *Phys. Rev. B* **61**, R16331 (2000).
- <sup>32</sup>W.-H. Chang, T.M. Hsu, C.C. Huang, S.L. Hsu, C.Y. Lai, N.T. Yeh, T.E. Nee, and J.-I. Chyi, *Phys. Rev. B* **62**, 6959 (2000).
- <sup>33</sup>J.J. Finley, A.D. Ashmore, A. Lemaître, D.J. Mowbray, M.S. Skolnick, I.E. Itskevich, P.A. Maksym, M. Hopkinson, and T.F. Krauss, *Phys. Rev. B* **63**, 073307 (2001).
- <sup>34</sup>K.F. Karlsson, E.S. Moskalenko, P.O. Holtz, B. Monemar, W.V. Schoenfeld, J.M. Garcia, and P.M. Petroff, *Appl. Phys. Lett.* **78**, 2952 (2001).
- <sup>35</sup>O.B. Shchekin and D.G. Deppe, *Appl. Phys. Lett.* **80**, 3277 (2002).